INTEGRATION OF THE OPTICAL REPLICA ULTRASHORT ELECTRON BUNCH DIAGNOSTICS WITH THE HIGH-RESOLUTION COHERENT OPTICAL TRANSITION RADIATION IMAGER

G. Geloni, P. Ilinski, E. Saldin, E. Schneidmiller and M. Yurkov, DESY, Hamburg, Germany

Abstract

Electron bunch imagers based on incoherent OTR constitute the main device presently available for the characterization of ultrashort electron bunches in the transverse direction. One difficulty to obtain high-resolution images is related with the very peculiar particle-spread function of OTR radiation, which has a large width compared to the usual point-spread function of a point-like source. In this contribution we explore the possibility of using coherent OTR instead of incoherent OTR radiation, by integrating an ORS setup with a high-resolution coherent optical transition radiation imager. Electron bunches are modulated at optical wavelengths in the ORS setup. When these electron bunches pass through a metal foil target, coherent radiation pulses of tens MW power are generated. It is thereafter possible to exploit the large number of available coherent photons. In particular we manipulate the particle spread function of the system, so that the imaging problem can be reduced to the usual (coherent or incoherent) imaging theory for point-like radiators. **These proceedings are based on the article [1], to which we address the interested reader for further information and references.**

INTRODUCTION

In this paper we present a feasibility study for integrating the ORS setup with a high-resolution electron bunch imager based on coherent Optical Transition Radiation (OTR). Our ideas are discussed in detail in [1], where the interested reader will also find relevant references that are omitted here for reasons of space.

The need for high-resolution coherent OTR imagers as diagnostic tools is due to the extreme characteristics of the electron beams in XFELs, where the ability of monitoring the spatio-temporal structure of sub-100 fs electron bunches as they travel along the XFEL structure becomes of great importance.

The main advantages of coherent OTR imaging with respect to the usual incoherent OTR imaging is in the coherence of the radiation pulse, and in the high photon flux. In this work we restrict ourselves to issues related to the integration of coherent OTR imagers with the ORS setup. This procedure, eventually opens up the possibility of single-shot, 3D imaging of electron bunches with microscale resolution, which have been described elsewhere in these Proceedings.

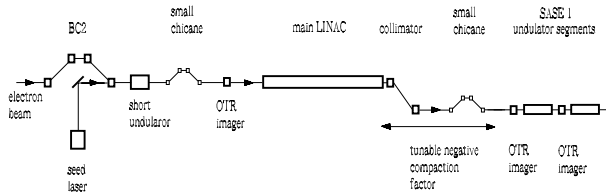

Figure 1: Schematic diagram of the coherent imager. The working principle is based on the optical modulation of the electron bunch and on emission of coherent OTR radiation from the metallic mirror.

OPTICAL REPLICA SETUP

We propose to create a coherent pulse of optical radiation by modulating the electron bunch at a given optical wavelength and by letting it pass through a metal foil target, thus producing coherent OTR at the modulation wavelength. The radiation pulse should be produced in such a way to constitute an exact replica of the electron bunch. The optical replica can be used for the determination of the 3D structure of electron bunches. Although other projects may benefit from our study too, throughout this paper we will mainly refer to parameters and design of the European XFEL.

In order to produce the optical replica we need to modulate the electron bunch at a fixed optical wavelength. One may take advantage of an Optical Replica Synthesizer (ORS) modulator, which we suppose to be installed after the BC2 bunch compressor chicane.

A method for peak-current shape measurements of ultrashort electron bunches using the undulator-based Optical Replica Synthesizer (ORS), together with the ultrashort laser pulse shape measurement technique called Frequency-Resolved Optical Gating (FROG) was recently proposed (see references in [1]). It was demonstrated that the peak-current profile for a single, ultrashort electron bunch could be determined with a resolution of a few femtoseconds. The ORS method is currently being tested at the Free-electron laser in Hamburg (FLASH). Novel results will be reported at this conference (see THOB02).

A basic scheme to generate coherent OTR is shown in Figure 1.

A relatively long laser pulse serves as a seed for the modulator, consisting of a short undulator and a dispersion section. The central area of the laser pulse should overlap with the electron pulse. In order to ensure simple synchronization, the duration of the laser pulse should be much longer than the electron pulse time jitter, which is estimated to be of order 100 fs. Foreseen parameters of the seed laser are: wavelength $\lambda_m = 800$ nm, energy in the laser pulse 1 mJ and pulse duration (FWHM) 1 ps. The laser beam is focused onto the electron bunch in a short (the number of periods is $N_w = 5$) modulator undulator resonant at the optical wavelength of 800 nm. Optimal conditions of focusing are met by positioning the laser beam waist into the center of the modulator undulator, with a Rayleigh length of the laser beam equal to the undulator length. Since the electron betatron function β, the undulator length L_w and the Rayleigh length of the laser beam are of the same magnitude, the size of the laser beam waist turns out to be about 20 times larger than the electron beam size. As a consequence, we can approximate the laser beam with a plane wave when discussing about the modulation of the electron bunch. The seed laser pulse interacts with the electron beam in the modulator undulator and produces an amplitude of the energy modulation in the electron bunch of about 500 keV. Subsequently, the electron bunch passes through the dispersion section (with momentum compaction factor $R_{56} \simeq 50\mu$m), where the energy modulation is converted into density modulation at the laser wavelength. The electron bunch density modulation reaches an amplitude of about 10%. Finally, the modulated electron bunch travels through the OTR screen. It should be mentioned that OTR screens can be positioned at various locations down the electron beam line where electrons have substantially different energies. In the case of the European XFEL, the electron energy varies from 2 GeV (second bunch compression chicane) up to 17.5 GeV at the undulator entrance. For other machines, these parameters differ. In the case of LCLS, energies will range from about 4.5 GeV to 13.6 GeV.

In the case the OTR screen is placed downstream the main Linac, self-interactions and in particular longitudinal space-charge (LSC) interactions become important. As one may see from Fig. 2, due to LSC interactions the bunch density modulation after the Linac depends on the current level. This constitutes a detrimental effect concerning our imaging techniques, because the peak-current along the bunch is not constant, so that the modulation level varies along the bunch in a complicated way depending on the variation of the peak-current level. This effect is unwanted. In fact, different parts of the electron bunch should be given the right weight as concerns their contribution to radiation emission, meaning that the (absolute) charge modulation in each point of the electron bunch should be proportional to the charge density distribution of the unmodulated bunch. This can only be realized when the bunching factor is uniform along the bunch i.e. when it does not depend on the charge density distribution nor on the energy spread distribution.

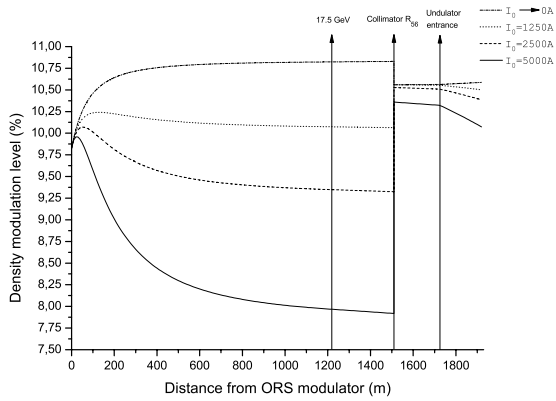

Figure 2: Evolution of the level of the electron bunch density modulation for different values of the peak-current I_0. Here we account for the presence of a dispersive element $R_{56}^{(c)} \simeq 12\mu$m at the collimation system.

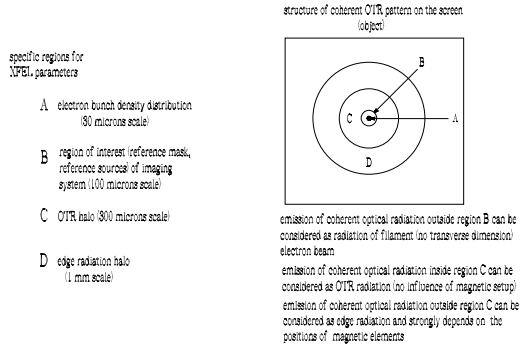

Figure 3: Scheme of the coherent OTR radiation pattern as observed in the object plane for the low electron beam energy case of 2 GeV.

Insertion of a small chicane (with positive R_{56}) allows one to organize, together with the collimation section, a dispersive element with tunable, negative R_{56}. This allows to compensate the positional-dependent variations of the electron bunch density modulation level, as shown in Fig. 2. Reference [1] includes a thorough discussion about this compensation scheme.

THE OTR SOURCE

A powerful burst of OTR is emitted, which contains coherent and incoherent parts. The coherent OTR has much greater number of photons, up to 10^{13} i.e. 1μJ per pulse. A detailed study shows that, in our case of interest, we can exploit the Ginzburg-Frank formula for the characterization of the OTR field from a single electron at the OTR screen. Then, the field distribution for the electron bunch at the OTR screen in the space-frequency domain is essentially a convolution in the space domain of the temporal Fourier transform of the charge density distribution and the tem-

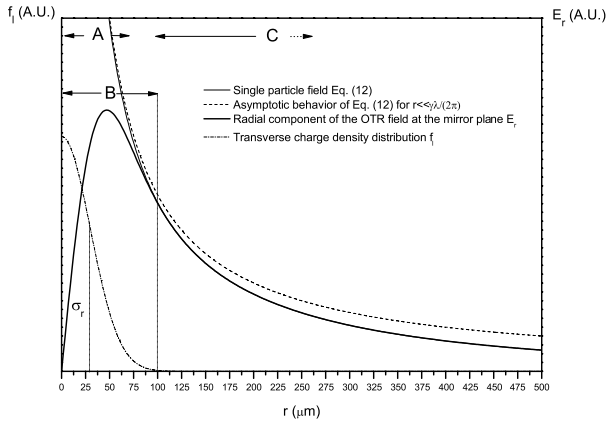

Figure 4: Radial component of the OTR field in the mirror plane, transverse (Gaussian) charge density distribution f_l, single particle field, scaling as $2\pi K_1[2\pi r/(\gamma\lambda)]/(\gamma\lambda)$, and its asymptote for $r \ll \gamma\lambda/(2\pi)$ scaling as $1/r$. Here the electron energy is 2 GeV, the electron bunch transverse rms size is $\sigma_r = 30$ μm, the modulation wavelength is, as usual $\lambda = 800$ nm.

poral Fourier transform of the single-electron field. Qualitatively, we can distinguish between four zones of interest, Fig. 3. Information about the electron bunch will be shown to be included in a small region of size $\sigma_r \sim 30\mu$m, region A. The region of interest of the imaging system is characterized by $r < 100$ μm, region B. The field distribution for 100 μm $< r < 300$ μm does not depend on the transverse size of the electron beam, region C. Finally, the position of magnetic structures become relevant at larger distances $r \sim 300$ μm $\sim \gamma\lambda/(2\pi)$, region D. An example of convolution between single-particle field and transverse charge density distribution (in the space-frequency domain) is given in Fig. 4 in the case of a gaussian transverse density distribution. The different zones of interest can be identified by inspection.

COHERENT OTR IMAGING

The so called $4f$ filtering architecture is ideal for a coherent OTR imaging setup, Fig. 5. In [1], we demonstrated that such setup can be used to characterize electron density profiles on the microscale level. Such resolution level can be reached, for example, by spatially filtering in the Fourier plane and using a radial-to-linear polarization converter. In this way, the particle spread function is improved up to the point spread function for a point-like source.

Figure 6 shows the response of a simple two-lens setup in the case of OTR emitted by a single electron, which is given by

$$A_p(\omega, r_i) = \frac{\theta_a}{\gamma^2} \cdot \frac{1 - J_0(\omega r_i \theta_a / c)}{\omega r_i \theta_a / c} , \qquad (1)$$

for $r_i \ll \gamma\lambda/(2\pi)$, θ_a being the numerical aperture of the lens. The response is due to the specific characteristics of

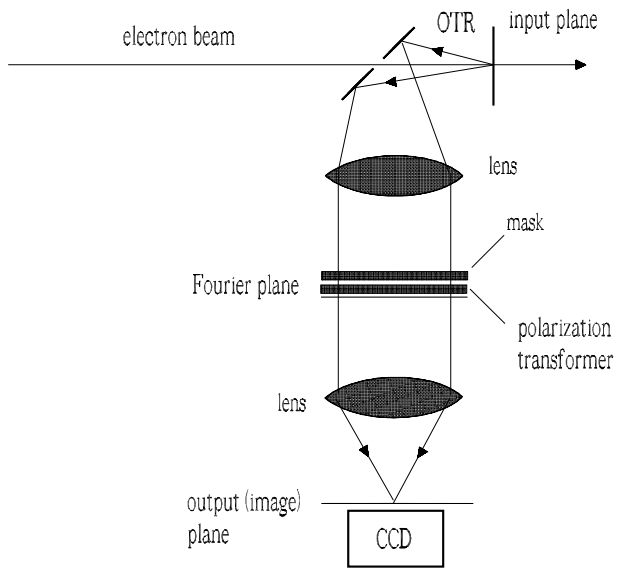

Figure 5: A practical arrangement of the coherent OTR image-processing system (the hole in the OTR screen is for simplicity of drawing only. A tilted configuration should be used at these wavelengths instead).

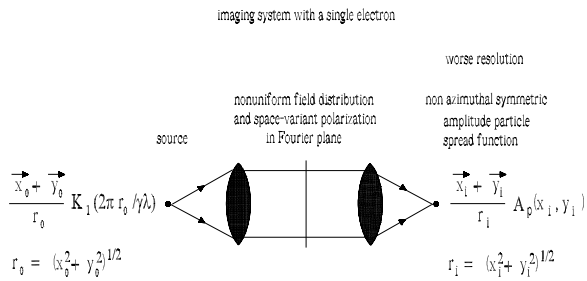

Figure 6: The response of the system in the case of Optical Transition Radiation emitted by a single electron.

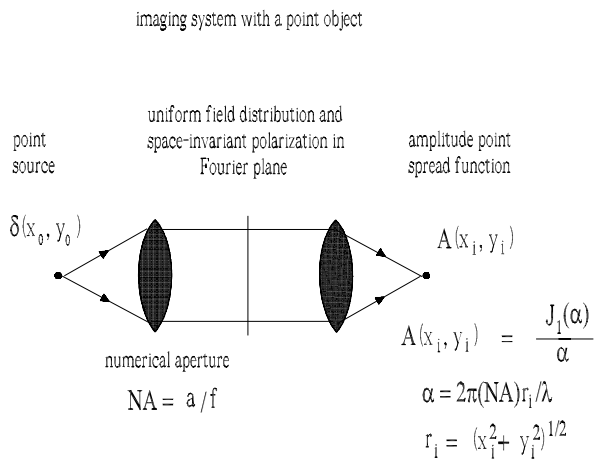

Figure 7: Two-lens imaging system with a point source.

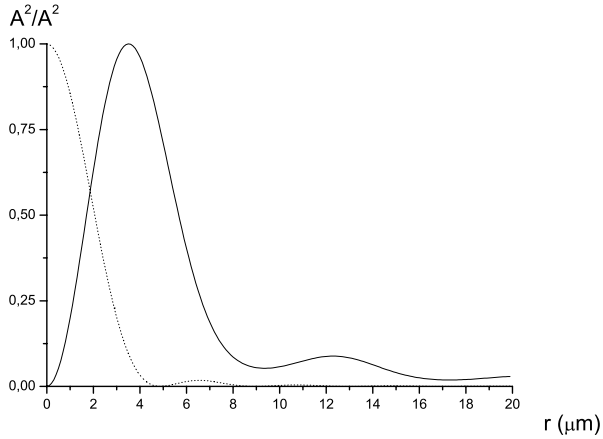

Figure 8: The particle spread function of the system (solid line), A_p^2 in Eq. (1), for $\lambda = 800$ nm and $\theta_a = 0.1$. The point spread function, for which $A^2 = \lambda^2 J_1^2[2\pi r_i \theta_a/\lambda]/(2\pi r_i \theta_a)^2$, is shown for comparison (dashed line).

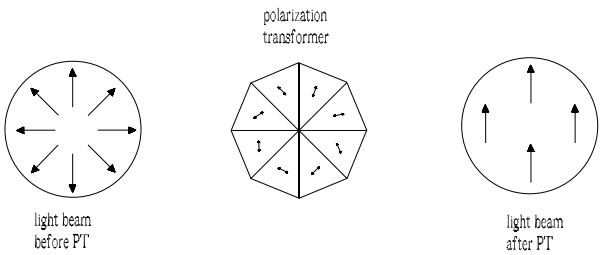

Figure 9: Schematic plot illustrating the transformation of a radially polarized beam into a linearly polarized beam. Instead of a continuous spatially varying retarder, a sectioned device can be used, where each section has different orientation of the optical axis of the half-wave plate.

OTR. Figure 7 shows instead, the response of the same two-lens setup in the case of a point source. The difference between the two response functions is further illustrated in Fig. 8. As one can see a decreased resolution is to be expected, with respect to the case of point-like sources, due to the particular nature of the OTR response.

Use of a Fourier-plane mask with transmission function $T_m(r) = T_0 r/a$ (where T_0 is a common-amplitude attenuation coefficient, and a is the pupil size) and a polarization transformer made of several half-wave plates with different orientations of the optical axis (see Fig. 9 and references [43] and [44] in [1]) allows one to get back to the case shown in Fig. 7, where the field in the focal plane is uniform, and the polarization is spatially invariant.

As a result, one improves the OTR particle spread function to obtain the usual point spread function. Our scheme can be implemented in an OTR imaging system as shown

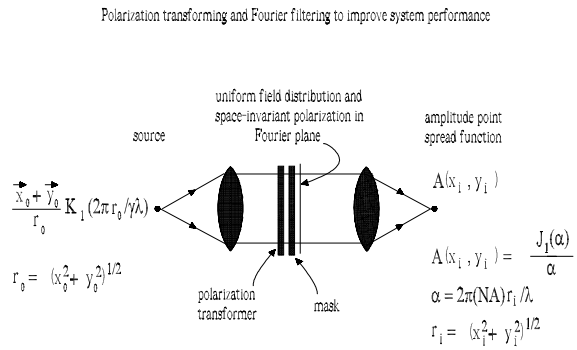

Figure 10: OTR particle spread function synthesis by a Fourier-plane filter and a polarization transformer.

in Fig. 10. This scheme is an example of exploitation of the large number of coherent photons from a coherent OTR setup. It should be noted that the coherent OTR pulse produced integrating the ORS setup with an OTR screen is an actual replica of the electron bunch. Thus, once the coherent OTR pulse is characterized in three dimensions, also the electron bunch is. Based on this observation, elsewhere in these Proceedings (WEPC47) and in [1], we propose several concepts to reach the final goal of full three-dimensional characterization of ultrashort, relativistic electron bunches. They all rely on the integration of the optical replica ultrashort electron bunch diagnostics with a high-resolution coherent optical transition radiation imager.

REFERENCES

[1] G. Geloni, P. Ilinski, E. Saldin, E. Schneidmiller and M. Yurkov, "Method for the determination of the three-dimensional structure of ultrashort relativistic electron bunches", DESY 09-069, online version at http://arxiv.org/abs/0905.1619